Age-dependent loss of mitochondrial DNA integrity in mammalian muscle

Paulina H. Wanrooij[1,*], Phong Tran[1], Liam J. Thompson[2], Sushma Sharma[1], Katrin Kreisel[2], Clara Navarrete[2], Anna-Lena Feldberg[1], Danielle Watt[1], Anna Karin Nilsson[1], Martin K. M. Engqvist[2,3], Anders R. Clausen[2], and Andrei Chabes[1,4,*]

[1]Department of Medical Biochemistry and Biophysics, Umeå University, 901 87 Umeå, Sweden; [2]Institute of Biomedicine, University of Gothenburg, 405 30 Gothenburg, Sweden; [3]Department of Biology and Biological Engineering, Chalmers University of Technology, 412 96 Gothenburg, Sweden; [4]Laboratory for Molecular Infection Medicine Sweden (MIMS), Umeå University, 901 77 Umeå, Sweden.

*Correspondence: paulina.wanrooij@umu.se or andrei.chabes@umu.se.

Running title: Progressive loss of muscle mtDNA integrity

Key words: mitochondrial DNA; mtDNA; genome stability; ribonucleotide incorporation; dNTP pool.

Summary

MtDNA integrity is important for mitochondrial function. We analysed mtDNA over the course of mouse lifespan and found that its integrity, as measured by electrophoretic mobility under denaturing conditions, decreased significantly in old animals whereas its ribonucleotide (rNMP) content increased with age. To investigate whether the rNMPs incorporated into mtDNA were responsible for this loss of integrity in old animals, we used mice deficient in SAMHD1, a dNTPase that decreases rNTP/dNTP ratios. Knockout of SAMHD1 almost completely eliminated rNMPs from mtDNA, but did not restore mtDNA integrity in older animals, indicating that rNMP incorporation does not explain the loss of mtDNA integrity. Neither did mtDNA from older animals contain more gaps, deletions or double-strand breaks than that of younger animals. By contrast, mtDNA integrity was restored by treatment with ligase. Thus, we conclude that the loss of mtDNA integrity in old mice is caused by accumulation of nicks.

Introduction

The genome of mitochondria in mammalian cells is a circular 16 kb dsDNA molecule present in multiple copies per cell. This mitochondrial (mt)DNA encodes key subunits of the respiratory chain complexes that synthesize the majority of the cell's ATP. Consequently, a partial loss of the number of copies of mtDNA from the cell (i.e. depletion) or defects in the quality of the DNA can affect energy production and manifest as human disease [1]. MtDNA quality also decreases with age due to the progressive accumulation of deletions and point mutations [2-4], which may contribute to the physiology of aging [5].

Ribonucleotides (rNMPs) incorporated into DNA are an important threat to genome stability. Although replicative DNA polymerases are highly selective for dNTPs, the large excess of rNTPs over dNTPs in the cell results in incorporation of some rNMPs during DNA replication [6,7]. Due to their reactive 2'-hydroxyl group, these rNMPs increase the risk of strand breaks by several orders of magnitude [8]. Furthermore, the presence of rNMPs in DNA can alter its local structure and elasticity [9-11], thus interfering with processes such as replication, transcription or DNA repair. To prevent these negative effects of incorporated rNMPs on genome stability, they are removed from nuclear DNA (nDNA) by the ribonucleotide excision repair pathway, which is initiated by cleavage at the incorporated rNMP by RNase H2 [7,12]. RNase H2 is essential for genome stability in mammals and its absence results in increased single-stranded DNA (ssDNA) breaks and an activated DNA damage response [13,14].

In contrast to nDNA, mtDNA contains persistent rNMPs that are incorporated during replication by the mtDNA polymerase, Pol ɣ (reviewed in [15]). Human Pol ɣ is highly selective against using rNTPs as substrates and thus incorporates fewer rNMPs than nuclear replicative DNA polymerases do [16-18]. Once incorporated, however, rNMPs persist in mtDNA because mitochondria lack repair pathways for their removal [19,20]. Although a certain level of rNMPs is tolerated in mtDNA, it remains unclear whether higher levels might have harmful effects on mtDNA stability. Interestingly, the rNMP content of mtDNA is affected in cell lines from patients with mtDNA depletion syndrome (MDS) [20]. Also, aberrant rNMP incorporation is proposed to play a role in the mtDNA depletion and deletions observed in mice lacking the mitochondrial inner membrane protein MPV17 [21].

Considering the crucial importance of intact mtDNA for human health [1], we set out to investigate how the integrity of mtDNA might change during the lifespan of the mouse. We report here that mtDNA integrity, as defined by the median length of single-stranded mtDNA fragments determined by electrophoretic mobility under denaturing conditions, decreases in skeletal muscle during aging. Given the well-recognised negative impact of rNMPs on nDNA integrity, we asked whether rNMPs might contribute to the observed age-dependent fragmentation of muscle mtDNA. To this end, we used a mouse model that is deficient in the dNTP triphospohydrolase (dNTPase) SAMHD1 and that consequently has higher levels of dNTPs than wild-type (wt) mice. In accordance with the decreased rNTP/dNTP ratio in *SAMHD1*$^{-/-}$ skeletal muscle, we observed a considerable reduction in mtDNA rNMPs. This change, however, did not increase mtDNA integrity in aged animals, demonstrating that mtDNA rNMPs do not cause the age-related fragmentation of mtDNA. Because the integrity of the mtDNA was restored by treatment with ligase, we conclude that mtDNA accumulates single-stranded nicks over the course of the lifespan of the mouse, which may explain the age-related loss of mtDNA integrity.

Results

MtDNA integrity decreases with age

To examine mtDNA integrity during the lifespan of the mouse, we isolated total DNA from whole embryos and from the tibialis anterior (TA) muscle of mice at various ages, separated it on a denaturing gel and then visualized the mtDNA by Southern blotting using a double-stranded DNA (dsDNA) probe targeting both strands in a region of the *COX1* gene. Under denaturing conditions that separated the two DNA strands, skeletal muscle mtDNA from aged (2-year-old) mice migrated faster than that from adults (13 weeks old) or pups (15 days old), and the mtDNA from embryos migrated the most slowly (Fig. 1a). The length distribution of mtDNA in each sample lane was quantified relative to size markers run in parallel (Fig. S1a) and expressed as the apparent median length (Fig. 1b), thus providing a measure of the integrity of the single strands of mtDNA in the sample. The apparent median length (henceforth referred to as median length) of muscle mtDNA was reduced from 4,900 nt and 5,000 nt in pups and adults, respectively, to 3,200 nt in aged animals (Fig. 1b). A similar decrease in muscle DNA integrity with age was not observed when the blot shown in Fig. 1a was probed for nuclear 18S rDNA (Fig. S1b), indicating that the decrease in median length of the mtDNA was not due to nuclease contamination or other artefacts of sample preparation. To confirm that the difference in mtDNA integrity seen between adult and aged muscle was not introduced during DNA purification, we analysed highly purified mtDNA isolated by an alternative procedure that results in less DNA shearing, as indicated by the higher median length of mtDNA (compare Fig. S1d to Fig. 1b), but a much lower yield. The statistically significant difference between adult and aged mtDNA persisted (Fig. S1c, d), confirming that the age-dependent loss of integrity was not an artefact of sample preparation.

MtDNA deletions such as the 5 kb common deletion are known to accumulate during aging [3]. To investigate whether the observed short median length of mtDNA in aged muscle might be due to similar large mtDNA deletions or dsDNA breaks, the DNA was linearized with the SacI endonuclease and analysed on a neutral gel, where it migrated primarily as a band corresponding to the full-length (16.6 kb) mtDNA molecule (Fig. 1c). In addition, adult, old adult (1 year old) and aged skeletal muscle contained a more slowly migrating species that was absent in preparations from embryos and barely detectable in pups. This slower-migrating species may represent nicked circles that are resistant to digestion and/or higher-order mtDNA forms that are reported to accumulate in certain tissues during aging [22,23]. Importantly, the proportion of DNA that migrated faster than full-length mtDNA and thus comprises mtDNA molecules containing large deletions or dsDNA breaks did not increase progressively with age (Fig. 1c; Fig. S1e). Consistent with this, a sensitive, long-range PCR assay that preferentially amplifies mtDNA molecules with deletions revealed only a very small increase in such species in aged muscle (Fig. 1d). We conclude that the shorter median length of mtDNA observed in the muscle of aged mice, when compared to younger animals, cannot be attributed to an increase in mtDNA deletions or dsDNA breaks.

The rNMP content of mtDNA increases during lifespan and varies between tissues

Given that mitochondria lack effective pathways for removal of incorporated rNMPs [19,20,24-26] and that the presence of incorporated rNMPs renders the DNA backbone more prone to breakage [8], we investigated whether rNMPs might contribute to the observed loss of mtDNA integrity in skeletal muscle of aged mice. Alkali (KOH) treatment is commonly used to hydrolyse DNA at sites of rNMP incorporation. To validate that the extent of alkali sensitivity provides an accurate readout of the rNMP content of mtDNA, we treated samples from mouse

liver, heart and skeletal muscle either with alkali or with recombinant RNase HII, an enzyme that cleaves the DNA backbone at incorporated rNMPs, and analysed the resulting mtDNA on denaturing gels. Both treatments caused a similar, marked decrease in the median length of mtDNA fragments (Fig. S2a), confirming that mtDNA from these three tissues contains rNMPs and that most alkali-sensitive sites are rNMPs rather than abasic sites, which are also sensitive to KOH. Thus, we used alkali treatment in further experiments as an assay for rNMPs in mtDNA.

We examined the rNMP content of skeletal muscle mtDNA from mice of various ages by comparing the electrophoretic mobility of untreated and alkali-treated DNA on a denaturing gel. MtDNA from embryos was analysed in parallel. Alkaline hydrolysis resulted in substantially shorter mtDNA fragments than in the untreated samples from pups, adult and aged mice, whereas the mtDNA from embryos was much less affected (Fig. 2a). By comparing the median lengths of the DNA in the untreated and alkali-treated samples, we estimated the number of rNMPs incorporated per strand of mtDNA. Whereas the mtDNA from embryos contained very few incorporated rNMPs (~ 1 rNMP per strand of mtDNA), the number of rNMPs in skeletal muscle mtDNA increased from ~ 5 per strand in pups to 8.5 per strand in adult animals (Fig. 2b). No difference was observed, however, between the number of rNMPs in skeletal muscle of adult and aged mice, demonstrating that rNMP content does not increase in skeletal muscle during aging (Fig. 2a, b). The rNMP content of mtDNA from heart was also higher in adult mice (~ 5 rNMPs per strand) than in pups (~ 1 rNMP per strand) but, in contrast to the skeletal muscle, there was little difference between embryos and pups (Fig. S2b, c). Notably, there were fewer rNMPs in heart than in skeletal muscle in both pups and adult animals (compare Fig. 2b and Fig. S2c).

Intrigued by the observed difference in rNMP content in heart and skeletal muscle, we analysed mtDNA rNMP content in several tissues from adult mice by using the same alkaline hydrolysis assay. This revealed clear differences in mtDNA rNMP content between tissues (Fig. 2c, d). Spleen, heart and brain mtDNA contained ~ 6 rNMPs per strand of mtDNA, whereas liver and both the TA and gastrocnemius (GAS) muscles of the hind leg contained 10–12 rNMPs per strand. Stripping and re-hybridization of the *COX1* blot in Fig. 2c with a probe annealing to another region of the mtDNA – the D-loop, a triple-stranded region formed by stable incorporation of a short DNA strand known as 7S DNA – indicated that both regions have a similar rNMP content (Fig. S2d; quantification was not possible due to the interfering signal of the 7S DNA). Finally, Southern blot analysis using ssDNA probes revealed no apparent strand bias in rNMP content between the H- and L-strand of mtDNA (Fig. S2e). As expected, nDNA from the various tissues was not affected by alkaline hydrolysis (Fig. S2f).

Whereas some studies have found that the ratio of free rNTPs to dNTPs determines the frequency of rNMP incorporation into the mtDNA of the yeast *Saccharomyces cerevisiae* [19] and of cultured human cells [20], others have reported changes in mtDNA rNMP content that did not correspond to an alteration in rNTP/dNTP ratios [21]. We therefore sought to determine whether the differences in mtDNA rNMP content we observed in various tissues correlated with differing rNTP/dNTP ratios. We measured the levels of individual rNTPs and dNTPs in mouse embryos and in spleen and skeletal muscle from adult animals by high-performance liquid chromatography, and calculated the ratio of each rNTP to its corresponding dNTP (Table 1). Of the four rNTP/dNTP pairs, the rATP/dATP ratio was highest, in accordance with the abundance of rATP in most cell types [6,27], and it varied most between tissue types: embryonic tissue contained a 470-fold excess of rATP over dATP, in spleen there was an 800-fold excess and in skeletal muscle a 37,000-fold excess. This high ratio

observed in skeletal muscle greatly exceeds the ability of the mitochondrial DNA polymerase, Pol ɣ, to distinguish rATP from dATP (discrimination factor of 9,300-fold; [17]). The ratio of the other three rNTP/dNTP pairs varied considerably less between tissues and remained well below the value of the Pol ɣ discrimination factor for each pair [17]. The rATP/dATP ratio may therefore have the greatest impact on the rNMP content of mtDNA – indeed, the rNMP content of mtDNA appears to reflect the magnitude of the rATP/dATP ratio (Fig. 2d, Table 1) – providing a possible explanation for the varying mtDNA rNMP content in the different tissues.

Mice with elevated dNTP pools have fewer rNMPs in their mtDNA

We and others have previously demonstrated that mice deficient in the dNTP triphosphohydrolase SAMHD1 have elevated dNTP levels [28,29]. Since the mtDNA rNMP content correlates directly with the rATP/dATP ratio, we reasoned that mtDNA from *SAMHD1*$^{-/-}$ mice with increased dNTP levels should contain fewer rNMPs. To test our hypothesis, we first examined the rNMP content of skeletal muscle mtDNA from wildtype (wt) and *SAMHD1*$^{-/-}$ (ko) mice. The number of rNMPs in mtDNA from GAS and TA muscle of *SAMHD1*$^{-/-}$ animals was much lower than that of wt animals: fewer than 1 rNMP per strand in *SAMHD1*$^{-/-}$ compared to ~ 9 and ~ 8 in wt GAS and TA, respectively (Fig. 3a, b). By contrast, the mtDNA rNMP content of muscle from *SAMHD1*$^{+/-}$ heterozygotes was not significantly affected, in accordance with the mild effect of heterozygosity on their rNTP/dNTP ratios [28]. SAMHD1-deficiency had no effect on the sensitivity of nDNA to alkaline hydrolysis (Fig. S3a). An equally striking decrease in rNMP content was observed in the mtDNA from *SAMHD1*$^{-/-}$ liver, and it persisted in old adults (Fig. 3c, d; see Fig. S3b for nDNA blot). We also examined heart mtDNA from old adults and found fewer rNMPs in *SAMHD1*$^{-/-}$ than in wt (Fig. S3c–e), confirming the effect even in a tissue in which the rNMP content is low compared to skeletal muscle and liver.

To identify the rNMPs incorporated into the mtDNA of wt and *SAMHD1*$^{-/-}$ animals, we used the HydEn–seq method [30]. In this method, KOH-treated samples are sequenced to uncover the identity and relative proportions of the four individual rNMPs. Consistent with the high rATP/dATP ratio in most tissues (Table 1; [6,27]) and with previous reports on mtDNA from solid mouse tissues [21], the most commonly occurring rNMP in the mtDNA from the liver of wt animals was rAMP, which comprised ~ 60% of all rNMPs (Fig. 4a). In comparison, rGMP comprised ~ 20%, and rUMP and rCMP each comprised ~ 10% of the total incorporated rNMPs. In contrast, the relative proportion of each individual dNMP at random background nicks, as determined by sequencing of 5'-ends in untreated (KCl-treated) samples, was close to 25% (Fig. S4a). In *SAMHD1*$^{-/-}$ animals, mtDNA contains very few rNMPs (Fig. 3). Accordingly, the proportions of the four individual bases determined by HydEn-seq in the mtDNA of *SAMHD1*$^{-/-}$ animals approached 25% (Fig. 4a), similar to the proportions of dNMPs at random background nicks (Fig. S4a). The similar proportion of bases at alkali-induced ends and at 5'-ends suggests that the majority of the 'rNMPs' in the mtDNA of *SAMHD1*$^{-/-}$ animals are in fact random background nicks rather than actual rNMPs. In contrast to the mtDNA, deletion of SAMHD1 did not alter the identity of the rNMPs in nDNA (Fig. 4b). Like the mtDNA in *SAMHD1*$^{-/-}$ animals, the nDNA of wt and *SAMHD1*$^{-/-}$ mice contained virtually no rNMPs (Fig. S3b). Therefore, the data obtained for nDNA similarly represent a low level of 5'-ends due to random background nicks. Consistent with this interpretation, the proportion of each 'rNMP' in nDNA was ca. 25%, comparable to the proportion of each dNMP at 5'-ends as determined by 5'-end sequencing (Fig. S4b). Finally, we analysed the rNMPs incorporated into each individual strand of the mtDNA. No strand bias was found in the incorporation of rNMPs into

mtDNA from wt or *SAMHD1*$^{-/-}$ when analysed by HydEn–seq (Fig. 4c), in accordance with the Southern blot analysis (Fig. S2e). Similar analysis of nDNA showed no difference between the two strands (Fig. S4c). Taken together, these data suggest that the dNTP pool perturbations observed in *SAMHD1*$^{-/-}$ animals reduce both the amount of rNMPs incorporated into the mitochondrial genome and the relative proportion of rAMP incorporated.

Incorporated rNMPs do not cause the loss of mtDNA integrity in aged skeletal muscle

To investigate the involvement of incorporated rNMPs on the age-dependent loss of mtDNA integrity, we compared the effect of age on mtDNA in *SAMHD1*$^{-/-}$ animals, which we have shown above have low rNMP content in their mtDNA, to the effect in wt animals. First, we determined the effect of *SAMHD1* deletion on mtDNA copy number by quantitative real-time PCR and found a decrease with age in the muscle of both wt and *SAMHD1*$^{-/-}$ animals (Fig. 5a). The mtDNA copy number of adult *SAMHD1*$^{-/-}$ mice was slightly larger than in wt, whereas no difference was observed between old adult or aged *SAMHD1*$^{-/-}$ and wt animals. Similar results were obtained for liver mtDNA except that both adult and old adult *SAMHD1*$^{-/-}$ animals had a larger mtDNA copy number than had wt animals of the same age (Fig. S5a). These data suggest that dNTP pools may limit mtDNA copy number in the muscle and livers of adult but not aged animals. Alternatively, or in addition, the larger mtDNA copy number in adult *SAMHD1*$^{-/-}$ animals may reflect greater mtDNA stability due to the decreased rNMP content.

Next, we compared the mtDNA integrity and rNMP content of TA muscle from aged wt mice to that from *SAMHD1*$^{-/-}$ mice by denaturing gel electrophoresis and Southern blotting with a COX1 probe, as above (Fig. 5b). Alkaline hydrolysis had little effect on the mobility of the mtDNA in these aged *SAMHD1*$^{-/-}$ animals (Fig. 5b) and the calculated rNMP content of their mtDNA remained very low compared to that in wt (Fig. 5c; the control for nDNA is shown in Fig. S5b). Importantly, there was no significant difference in the median length of untreated mtDNA in the aged wt and *SAMHD1*$^{-/-}$ animals (Fig. 5b and d), indicating that mtDNA integrity was not affected by the loss of this gene. These findings demonstrate that the amount of rNMPs incorporated into the mitochondrial genome does not influence the age-related loss of mtDNA integrity in muscle. Furthermore, *SAMHD1*$^{-/-}$ and wt muscle had similar amounts of mtDNA molecules containing deletions (Fig. 5e), and the lifespans of *SAMHD1*$^{-/-}$ and wt mice were indistinguishable (Fig. S5c). Taken together, these data show that whereas increased dNTP levels in *SAMHD1*$^{-/-}$ somewhat increase the copy number of mtDNA and drastically reduce its rNMP content, this results in no apparent benefit with regard to mtDNA integrity in aged animals.

Accumulation of ligatable nicks explains the age-dependent loss of mtDNA integrity

Since the age-dependent loss of mtDNA integrity observed in Figure 1 is not caused by rNMPs incorporated into mtDNA, we sought to identify another DNA alteration that might be responsible for the observed increased mobility under denaturing conditions of mtDNA from aged animals. Since the majority of mtDNA from aged animals migrates as species of ≥ 16 kb under neutral conditions (Fig. 1c), we reasoned that the increased mobility under denaturing conditions may be due to an increase in either DNA nicks or gaps. To differentiate between the two, we treated the DNA preparations with mung bean nuclease, a ssDNA-specific endonuclease that digests at gaps but not at nicks [31], and looked for DNA double-strand breaks among the products of the nuclease-treated DNA by electrophoresis on a neutral gel (Fig. 6a). As controls, we included samples of adult muscle mtDNA that was either rendered single-stranded by denaturing at 95°C or nicked by treatment with RNase HII. Under

conditions in which the nuclease digested the ssDNA but did not affect the mobility of the nicked DNA (Fig. 6a, lanes 13–17), nuclease treatment had only a small effect on the migration of mtDNA from aged mice (Fig. 6a, compare lanes 4–6 with lanes 10–12). Plots of the length distribution of untreated and nuclease-treated adult or aged mtDNA were very similar, whereas the distribution of the ssDNA control was markedly affected by nuclease treatment (Fig. 6b). Thus, DNA gaps are unlikely to contribute significantly to the decreased integrity of muscle mtDNA during aging.

DNA nicks (ssDNA breaks) can be inflicted by numerous endogenous and exogenous agents including reactive oxygen species, which are especially abundant in mitochondria [32]. Furthermore, nicks may derive from unfinished repair of various types of DNA lesions if the DNA end processing or ligation steps are not completed in a timely manner. To determine whether the nicks observed in aged muscle mtDNA contained ligatable ends, we treated the DNA preparations with T4 DNA ligase and separated ligase-treated and untreated samples on a denaturing gel (Fig. 6c). Ligase treatment resulted in a substantial increase in the median length of mtDNA from skeletal muscle of aged mice, whereas the effect on mtDNA from adult skeletal muscle was more modest (Fig. 6c, d; median lengths are presented in Fig. S6a) as was that on the liver mtDNA from adult or aged animals (Fig. 6d; Fig. S6b, c). These findings demonstrate that the integrity of skeletal muscle mtDNA is compromised in aged animals mainly due to an increase in DNA nicks, the majority of which have ligatable DNA ends.

Discussion

Mitochondrial dysfunction is a hallmark of aging, and the age-dependent accumulation of mtDNA molecules containing deletions or point mutations is firmly established (reviewed in [33-35]). Moreover, a causal role for mtDNA alterations in aging is suggested by the premature aging phenotype of mtDNA mutator mice, which have a proofreading-deficient Pol ɣ [36-38]. In this study, we addressed how the integrity of mtDNA changes during lifespan by using the median length of mtDNA fragments separated under denaturing conditions as a read-out of mtDNA integrity. This approach detects the presence of ssDNA breaks (nicks or gaps), dsDNA breaks and large deletions; it has not previously been reported, to our knowledge, for the comparison of mtDNA from animals of different ages. We report here that the mtDNA from skeletal muscles of mouse progressively loses its integrity during aging. This age-dependent loss of mtDNA integrity cannot be explained by the accumulation of large deletions, dsDNA breaks or gaps. Rather, it is due to the accumulation of nicks during the life of the animal.

The accumulation of nicks in the mtDNA of aged animals might result from the incorporation of rNMPs, which have previously been reported to be present in large numbers in mtDNA [24-26] and, we demonstrate here, increase in number with age. It is well established that failure to remove rNMPs from the mammalian nuclear genome results in frequent ssDNA breaks, increased replication stress, and activation of the p53-dependent DNA damage response that leads to death during embryonic development [13,14]. Enigmatically, the cell tolerates the presence of a significant number of rNMPs in mtDNA [16,20]. This tolerance of rNMPs in mtDNA might be due to the multicopy nature of mtDNA, its slower rate of replication, as well as the reverse transcriptase activity of Pol ɣ that allows it to bypass single rNMPs in the DNA template more effectively than nuclear replicative polymerases do [16,17]. Although a certain level of rNMPs in mtDNA is well-tolerated, we hypothesized that their continuous presence during lifespan might have a negative impact on mtDNA integrity

through decreased bypass by Pol ɣ [16,17] and increased ssDNA breaks, explaining the effect of age on mtDNA integrity.

To investigate whether rNMPs contribute to the loss of mtDNA integrity in aged mice we turned to a mouse model that has high levels of dNTPs. We previously demonstrated that yeast strains with an overall increase in dNTP pools have much lower levels of rNMPs in their mtDNA than have wt yeast [19]; we hypothesized that the same might be true of mice that lack the SAMHD1 dNTPase [39], which results in an increase of all dNTPs [28,29]. As predicted, *SAMHD1*$^{-/-}$ mice had much less rNMP in their mtDNA in all tissues examined than had wt animals. This reduced rNMP content, however, did not improve mtDNA integrity in aged *SAMHD1*$^{-/-}$ animals. Thus, we conclude that the presence of rNMPs in mtDNA cannot account for the loss of mtDNA integrity we observe in aged animals. Furthermore, the lifespan of *SAMHD1*$^{-/-}$ animals was similar to their wt littermates, indicating that the 'normal' level of rNMPs in wt mtDNA is well-tolerated and the reduction in rNMP content observed in *SAMHD1*$^{-/-}$ animals has no overall positive impact on mtDNA integrity. Additionally, our results establish a clear relationship between the rATP/dATP ratio of the tissue and the rNMP content in mtDNA of normal mammalian tissues: skeletal muscle, which has a high rATP/dATP ratio had a ~ 8-fold higher rNMP content than embryos that have a low rATP/dATP ratio.

Since the presence of rNMPs in mtDNA does not account for the loss of mtDNA integrity in aged animals, other forms of DNA damage must contribute to this effect. We ruled out an accumulation of large deletions, dsDNA breaks and ssDNA gaps. By contrast, the results of DNA ligation indicate that DNA nicks (i.e. ssDNA breaks) with ligatable ends accumulate in the mtDNA from the skeletal muscle of aged animals. In principle, these accumulated nicks might be due to a higher rate of their generation and/or a lower rate of their ligation. Interestingly, previous studies suggest that a decline in mitochondrial ligase activity might contribute to the increased number of nicks in the mtDNA of aged animals. Mammalian ligase III, the DNA ligase that is essential for mtDNA maintenance [40,41], is located both in the nucleus and the mitochondria [42], but only its mitochondrial function is essential [43,44]. In addition to its role in mtDNA replication, ligase III contributes to base excision repair (BER) in the mitochondrial compartment, which repairs the bulk of the oxidative damage inflicted on mtDNA, including ssDNA breaks [45]. Interestingly, the overall rate of mitochondrial BER is limited by the ligation step catalysed by ligase III [46] and mitochondrial ligase activity is reported to decline with age in rodent brain, consistent with this being a factor in the loss of mtDNA integrity with age, although protein levels of ligase III were not affected in old animals [47,48]. Finally, reactive oxygen species increase with age (reviewed in [49]). Thus, levels of oxidative DNA damage may exceed the capacity of mitochondrial BER and ligase III to repair them in aged animals. These findings, when considered together with our evidence that most of the nicks in the skeletal muscle mtDNA of aged animals contain ligatable ends, suggest that insufficient ligase capacity might underlie the age-dependent decrease in mtDNA integrity we report here. Because mtDNA nicks are likely to interfere with mitochondrial gene expression and thus energy production, their accumulation might well contribute to the mitochondrial dysfunction observed in aging. It will be interesting to investigate whether increased mitochondrial ligase activity might counteract loss of mtDNA integrity and improve respiratory capacity in older animals.

Acknowledgements

This project was supported by grants from the Swedish Research Council (to A.C. and to A.R.C.), the Swedish Cancer Society (to A.C.), the Swedish Foundation for Strategic Research (to A.R.C.) and the Lars Hierta Memorial Foundation (to P.H.W.). P.H.W. was supported by grants from the Swedish Cancer Society and the Swedish Society for Medical Research. We acknowledge Dr. Carol Featherstone of Plume Scientific Communication Services for professional editing of the manuscript.

Author contributions

P.H.W., P.T. and A.C. designed the study; P.H.W., P.T., S.S., K.K., C.N., A.L.F., D.W. and A.K.N. carried out the experiments; P.H.W., L.J.T, S.S., M.K.M.E., A.R.C. and A.C. analysed the data; P.H.W. and A.C. wrote the paper; all authors read and edited the paper.

Figure legends

Figure 1. The median length of skeletal muscle mtDNA decreases with age. A) DNA isolated from embryos and from the TA muscle of 15-day-old (pup), 13-week-old (adult) or 2-year-old (aged) animals was separated by electrophoresis on a denaturing gel. MtDNA was visualized by Southern blotting with a dsDNA probe for a region of the *COX1* gene. Each sample lane corresponds to an individual mouse. Dotted lines represent the median length of mtDNA in each group determined as in Fig. 1b. **B)** The median length of the mtDNA from Fig. 1a was determined based on the signal distribution (Fig. S1a), and age groups were compared using Welch's t-test (n=4). The p-values of statistically significant deviations from the adult group are indicated. The line indicates the median. **C)** DNA isolated from embryos and from the TA muscle of pups, adults, 1-year-old (old) adults or aged animals was linearised with SacI restriction endonuclease and separated by electrophoresis on a neutral gel. MtDNA was visualized by Southern blotting as above. MtDNA from embryos and pups migrated as expected for full-length (FL) mtDNA, whereas mtDNA from older animals also contained a slower-migrating species (*) that may represent dimers or species resistant to digestion. The signal distribution was quantified and is plotted in Fig. S1e. **D)** Long-range PCR was performed to detect deletions in mtDNA isolated from the TA muscle of mice of various ages as in Fig. 1c. Full-length product is indicated (FL). Only minor species containing deletions are observed in the mtDNA from old adults and aged animals, as indicated by the vertical line on the right-hand side of the gel. The size of the bands in the DNA ladder are indicated in kb. See also Fig. S1.

Figure 2. The rNMP content of mtDNA varies during lifespan and across different tissues. A) DNA isolated from embryos and from the TA muscle of pups, adult or aged animals was left untreated (data also shown in Fig. 1a) or hydrolysed with alkali (KOH) at sites of rNMP incorporation. Samples were separated by electrophoresis on a denaturing gel and mtDNA was visualized by Southern blotting as in Fig. 1. Each sample lane corresponds to an individual mouse. The experiment was performed twice; a representative blot is shown. Dotted lines represent the median length of mtDNA fragments. **B)** The length difference between untreated and alkali-treated samples shown in Fig. 2a was used to compute the number of rNMPs per single-strand of mtDNA in the various samples. The p-values of statistically significant deviations from the adult rNMP content are indicated (Welch's t-test; n=4), and the line indicates the median. **C)** Untreated and KOH-treated DNA from various adult mouse tissues and from embryos was separated by electrophoresis on a denaturing gel and mtDNA was visualized by Southern blotting as above. Each sample lane represents an individual mouse. Three independent experiments were performed; a representative image is shown. Dotted lines represent the median length of mtDNA fragments. See Fig. S2d–f for images of the same blot with other probes. **D)** The length difference between untreated and alkali-treated samples from three separate experiments including the one shown in Fig. 2c was used to compute the number of rNMPs per single-strand of mtDNA in embryos and in various adult tissues. Each dot represents an individual mouse and the lines indicate the median for each tissue. The size of bands in the DNA ladder are indicated in kb. See also Fig. S2.

Figure 3. MtDNA from *SAMHD1*$^{-/-}$ mice contains very little rNMPs. A) Untreated and alkali-treated DNA from skeletal muscle of adult wt and SAMHD1-deficient mice was analysed by electrophoresis on a denaturing gel and mtDNA was visualized by Southern blotting as in Figs

1 and 2. Each sample lane corresponds to an individual mouse. The experiment was carried out twice; a representative image is shown. GAS, gastrocnemius; TA, tibialis anterior; wt, wild type; het, *SAMHD1*$^{+/-}$; ko, *SAMHD1*$^{-/-}$. Dotted lines represent the median length of DNA fragments. **B)** The length difference between untreated and alkali-treated mtDNA shown in Fig. 3a was used to compute the content of rNMPs per single-strand of mtDNA. The p-values of statistically significant deviations from the wt are indicated (Welch's t-test; n=3); the horizontal lines indicate the median for each group. **C)** Untreated or KOH-treated DNA from the livers of 13-week-old (adult) or 1-year-old (old) wt and SAMHD1-deficient mice was analysed by electrophoresis on a denaturing gel and mtDNA was visualized by Southern blotting as above. Each sample lane corresponds to an individual mouse. The experiment was performed three times; a representative experiment is shown. Het, *SAMHD1*$^{+/-}$; ko, *SAMHD1*$^{-/-}$. Dotted lines represent the median length of DNA fragments. **D)** The length difference between untreated and alkali-treated mtDNA shown in Fig. 3c was used to compute the number of rNMPs per single-strand of mtDNA. The p-values of statistically significant differences from the wt adult group are indicated (Welch's t-test; n=3), and the horizontal lines indicate the median for each group. The size of bands in the DNA ladder are indicated in kb. See also Fig. S3.

Figure 4. The proportions of different rNMPs in mtDNA is altered in *SAMHD1*$^{-/-}$ animals. The base identities of rNMPs incorporated in the mitochondrial and nuclear genomes from the liver of adult wt and *SAMHD1*$^{-/-}$ (ko) mice were analysed by HydEn-Seq. Three wt and 4 *SAMHD1*$^{-/-}$ mice were analysed. **A)** The proportion of each rNMP (rAMP, rUMP, rGMP and rCMP) as a % of the total rNMPs present in mtDNA was plotted for wt and *SAMHD1*$^{-/-}$ mice. Error bars represent standard deviation. **B)** The proportion of each rNMP as a % of the total rNMPs present in nDNA was plotted for wt and *SAMHD1*$^{-/-}$ mice. Error bars represent standard deviation. **C)** The proportion (%) of each rNMP in each mtDNA strand (H, L) in wt and ko mice. Error bars represent standard deviation. See also Fig. S4.

Figure 5. The effect of increased dNTP pools and decreased rNMPs on mtDNA. A) MtDNA copy number in the TA muscle of 5 or 6 wt (filled dots) and *SAMHD1*$^{-/-}$ (open dots) 13-week-old (adult), 1-year-old (old) and 2-year-old (aged) animals was determined by qPCR and normalised to the value for adult wt. The mean for each group is indicated by a horizontal line. The p-values were calculated by using Welch's t-test; ns, non-significant. **B)** Untreated or alkali-treated DNA from skeletal muscle of wt and *SAMHD1*$^{-/-}$ (ko) mice was analysed by electrophoresis on a denaturing gel and mtDNA was visualized by Southern blotting as in Figs 1–3. Each sample lane corresponds to an individual mouse. Dotted lines represent the median lengths of DNA fragments in each group. **C)** The length difference between untreated and alkali-treated mtDNAs shown in Fig. 5b was used to compute the number of rNMPs per single-strand of mtDNA. The horizontal lines indicate the median for each group. The p-value of the statistically significant difference between the two groups was calculated by Welch's t-test; n=4. **D)** The median length of the untreated mtDNA in samples from Fig. 5b is indicated by a horizontal line. The two groups were compared using Welch's t-test (ns, non-significant; n=4). **E)** Long-range PCR was performed on mtDNA isolated from the TA muscle of adult and aged wt or SAMHD1$^{-/-}$ (ko) mice. FL, full-length product; the vertical line indicates the size range of mtDNA molecules with deletions. The size of bands in the DNA ladder are indicated in kb. See also Fig. S5.

Figure 6. MtDNA from aged animals contains many ligatable nicks. A) Untreated DNA (lanes 1–6) or mung bean nuclease-treated DNA (MBN; lanes 7–12) from the TA muscles of three adult (lanes 1–3 and 7–9) and aged mice (lanes 4–6 and 10–12) was separated by electrophoresis on a neutral gel and mtDNA was visualized by Southern blotting as in Figs. 1–3 and Fig. 5. As controls, samples of DNA from an adult (lane 17) were either rendered single-stranded by boiling (lanes 13–14) or were treated with RNase HII to introduce single-strand nicks in the mtDNA (lanes 15–16); and then treated with mung bean nuclease or left untreated, as indicated. **B)** DNA size distribution of the untreated (blue lines) and mung bean nuclease-treated (red lines) samples from Fig. 6a. The plots for adult and aged groups show the average of the three samples shown in Fig. 6a. **C)** Untreated DNA (lanes 1–3 and 7–9) or DNA treated with T4 DNA ligase (lanes 4–6 and 10–12) from adult (lanes 1–6) and aged mice (lanes 7–12) was separated by electrophoresis on a denaturing gel and mtDNA was visualized by Southern analysis as above. Dotted lines represent the median length of DNA fragments in each group. The median length of individual samples is plotted in Fig. S6a. **D)** The fold change in mtDNA length upon ligase-treatment of the samples in Fig. 6c (TA) or in Fig. S6b (liver); the length of untreated mtDNA was set to 1. The horizontal lines indicate the median for each group. The median lengths of untreated and ligase-treated TA and liver samples are plotted in Fig. S6a, c. The size of bands in the DNA ladder are indicated in kb. See also Fig. S6.

Tables

Table 1. rNTP/dNTP ratios from mouse embryos, adult spleen and skeletal muscle. The mean and standard deviation of three or four independent samples is given.

	rCTP/dCTP	rUTP/dTTP	rATP/dATP	rGTP/dGTP
Embryo	38.7 ± 6.02	53.5 ± 4.30	473 ± 36.3	208 ± 23.3
Spleen	14.4 ± 3.79	36.0 ± 10.3	806 ± 225	189 ± 62.6
Muscle	153 ± 67.0	139 ± 39.3	37 600 ± 13 300	226 ± 43.4

Methods

Animal handling and isolation of embryos and tissues

All mice were maintained at the animal facility at Umeå University under pathogen-free conditions. Mice were housed in an environment with a 12 hours dark/light cycle and *ad libitum* access to food and water. Animal handling and experimental procedure were approved by the ethical committee at Umeå University, complying with the rules and regulations of the Swedish Animal Welfare Agency and with the European Communities Council Directive of 22 September 2010 (2010/63/EU). All efforts were made to minimize animal suffering and to reduce the number of animals used. The lifespan study was conducted on 18 wt and 18 *SAMHD1*$^{-/-}$ mice. Mice were monitored throughout their life and humanely sacrificed once they reached moribund state. The survival of wildtype vs knockout animals was compared using the Mantel-Cox test in GraphPad Prism.

For collection of embryos at embryonic day 13.5, the dams were euthanised by cervical dislocation. The uteri were dissected on a petri plate containing ice-cold PBS. The tails of the embryos were isolated for genotyping and the embryos were snap-frozen in liquid nitrogen. The samples were stored at -80° C. As for tissues, mice with genotypes of interest were euthanised by CO_2 inhalation at the following ages: 15 days ('pup'), 13–16 weeks ('adult'), 1 year ('old adult') or 23–29 months ('aged'). The spleens, livers, hearts, brains and hind leg muscles (gastrocnemius [GAS] and tibialis anterior [TA]) were placed in Eppendorf tubes, quickly frozen in liquid nitrogen and kept at -80°C. Samples from an equal number of male and female animals were used in each experiment, as far as possible.

DNA isolation from embryos and tissues

Individual mouse tissues or whole embryos were incubated overnight with proteinase K (#P6556, Sigma), and total DNA (i.e. nDNA and mtDNA) was isolated according to standard protocols [50].

For the pure mtDNA in Fig. S1c-d, the TA muscle was minced into small pieces, washed in PBS containing 10 mM EDTA, and incubated with 0.05% trypsin in PBS with 10 mM EDTA for 90 min on ice. After centrifugation (200 × *g*, 5 min, 4°C), the pelleted tissue was resuspended in homogenization buffer (HB; 225 mM mannitol, 75 mM sucrose, 10 mM Hepes-KOH pH 7.8, 10 mM EDTA) and homogenized by 10 strokes of a Teflon-coated pestle. Nuclei and cell debris were pelleted at 800 × *g* for 10 min at 4°C and the supernatant was further centrifuged at 12,000 × *g* for 10 min at 4°C to pellet mitochondria. The mitochondria were resuspended in HB, overlaid on a sucrose gradient consisting of 1 M and 1.5 M sucrose in gradient buffer (10 mM Hepes pH 7.4 and 10 mM EDTA), and centrifuged at 40,000 × *g* for 1 h at 4°C. The purified mitochondria were diluted in gradient buffer, pelleted by centrifugation at 12,000 × *g* for 10 min at 4°C, resuspended in HB buffer containing 100 ng/µl proteinase K and incubated for 15 min on ice. Mitochondria were pelleted (12,000 × *g*, 10 min, 4°C), resuspended in lysis buffer (75 mM NaCl, 50 mM EDTA, 1% SDS, 20 mM Hepes pH 7.8) containing 100 ng/µl proteinase K, and incubated on ice for 30 min. MtDNA was purified by phenol–chloroform extraction followed by ethanol precipitation.

DNA treatments, agarose gel electrophoresis and Southern blotting

Where indicated, DNA preparations were digested overnight with the SacI restriction endonuclease followed by treatment with 20 µg RNase A (Thermo Scientific) in the presence of 300 mM NaCl, ethanol precipitation, and resuspension in TE buffer (10 mM Tris-HCl pH 8.0, 10 mM EDTA). Treatment with mung bean nuclease (New England Biolabs #M0250S; at 0.3

U/µg of DNA) was for 15 min at room temperature. T4 DNA ligase treatment (Thermo Scientific #EL0011; at 3.3 U/µg of DNA) was carried out at 25°C for 6 h, followed by inactivation at 65°C for 10 min in the presence of 25 mM EDTA and 0.2% SDS. For estimation of rNMP content, DNA was treated with 0.3 M KOH or with RNase HII as previously described [19].

DNA was separated by electrophoresis on 0.7% agarose gels under either neutral (1 × TAE buffer) or denaturing (30 mM NaOH and 1 mM EDTA) conditions at 1.2 V/cm for 16 h at 8°C; GeneRuler 1 kb DNA ladder (Thermo Scientific) was used as a standard for DNA length. The DNA was transferred to a nylon membrane using standard protocols [50] and probed sequentially with selected α-dCTP^{32}-labelled dsDNA probes, stripping extensively with boiling 0.1% SDS between probes. The probes used were *COX1* (nt 5,328–6,872) and D-loop (nt 15,652–15,679) for mouse mtDNA, and 18S (nt 1,245–1,787 of the 18S rRNA on chromosome 6 [gi 374088232]) for nDNA. In Fig. S2e, strand-specific probes targeting a region of *ND4* (nt 10,430–10,459) in mtDNA were used. Blots were exposed to BAS-MS imaging plates (Fujifilm), scanned on a Typhoon 9400 imager (Amersham Biosciences), and the signal was quantified by using ImageJ64 software. The apparent median length of DNA fragments and the rNMP content of mtDNA were determined from the length distributions of untreated and alkali-treated DNA samples as previously described [19]. Because the rNMP content of each individual sample was determined by comparing the median length of untreated vs. alkali-treated aliquots of the same sample, it was not affected by variation in DNA shearing during sample preparation. Data sets for median length and rNMP content were assessed for a normal distribution by using the Shapiro–Wilk test in GraphPad Prism software; all tested sample sets passed this test. Statistical comparisons between two groups were performed by using Welch's unequal variances t-test; each group contained 3 to 6 animals.

MtDNA deletion analysis by long-range PCR

The Expand Long Template PCR system (Roche) with forward and reverse primers at nt 2,478–2,512 and nt 1,906–1,933, respectively, was used to amplify a *ca.* 15,800 bp fragment of mouse mtDNA from 25 ng of total DNA. The cycling conditions were: 92°C 2 min, 30 cycles of (92°C 10 sec, 67°C 30 sec, 68°C 12 min), 68°C 7 min, 4°C hold. Products were separated by electrophoresis on a 0.7% agarose gel run in 1 × TAE buffer at 55 V in the cold room, and imaged on a ChemiDoc Touch instrument (Bio-Rad).

MtDNA copy number analysis by qPCR

MtDNA copy number was analysed in duplicate by quantitative real-time PCR using 2 µl of 1/400-diluted SacI-treated total DNA in a 10 µl reaction containing 0.2 µM forward and reverse primers and 1 x KAPA SYBR FAST qPCR Master Mix for LightCycler 480 (KAPA Biosystems) in a LightCycler 96 instrument (Roche). Primer pairs targeting cytochrome B (nt 14,682–14,771 of mtDNA [51]) and actin (nt 142,904,143–142,904,053 of chromosome 5 [NC_000071]) were used with the following qPCR program: 95°C 180 sec, 40 cycles of (95°C 10 sec, 57°C 10 sec, 72°C 1 sec with signal acquisition), melting curve (95°C 5 sec, 65°C 60 sec, heating to 97°C at 0.2°C/sec with continuous signal acquisition). C_q values determined by the LightCycler 96 software (Roche) were used to calculate the copy number of mtDNA relative to nuclear DNA using the Pfaffl method [52] and plotted with GraphPad Prism. Statistical comparisons between two groups were performed by using Welch's unequal variances t-test. Five to eight mice were analysed per genotype.

Mapping of 5'-ends and rNMPs

5'-ends in mtDNA and nDNA from mouse liver were mapped by 5'-End-seq by treating 1 µg total DNA with 0.3 M KCl for 2 h at 55°C. Ribonucleotides were mapped by HydEn-seq [30] by hydrolyzing 1 µg total DNA with 0.3 M KOH for 2 h at 55°C. Afterwards, ethanol-precipitated DNA fragments were treated for 3 min at 85°C, phosphorylated with 10 U of phosphatase-minus T4 polynucleotide kinase (New England BioLabs) for 30 min at 37°C, heat inactivated for 20 min at 65°C and purified with HighPrep PCR beads (MagBio). Phosphorylated products were treated for 3 min at 85°C, ligated to oligo ARC140 [30] overnight at room temperature with 10 U of T4 RNA ligase, 25% PEG 8000 and 1 mM $CoCl_3(NH_3)_6$, and purified with HighPrep PCR beads (Mag-Bio). Ligated products were treated for 3 min at 85°C. The ARC76±ARC77 adaptor was annealed to the fragments for 5 min at room temperature. The second strand was synthesized with 4 U of T7 DNA polymerase (New England BioLabs) and purified with HighPrep PCR beads (MagBio). Libraries were PCR-amplified with KAPA HiFi Hotstart ReadyMix (KAPA Biosystems), purified, quantified with a Qubit fluorometric instrument (ThermoFisher Scientific) and 75-base paired-end sequenced on an Illumina NextSeq500 instrument to locate the 5'-ends.

Sequence trimming, filtering, and alignment

All reads were trimmed for quality and adaptor sequence with cutadapt 1.12 (-m 15 -q 10 –match-read-wildcards). Pairs with one or both reads shorter than 15 nt were discarded. Mate 1 of the remaining pairs was aligned to an index containing the sequence of all oligos used in the preparation of these libraries with bowtie 1.2 (-m1 -v2), and all pairs with successful alignments were discarded. Pairs passing this filter were subsequently aligned to the mm10 *M. musculus* reference genome (-m1 -v2 –X2000). Single-end alignments were then performed with mate 1 of all unaligned pairs (-m1 -v2). Using the –m1 setting causes Bowtie to discard all reads which align to multiple places in the genome, including nuclear mitochondrial DNA segments (NUMTs). To calculate the base identity of 5'-ends or rNMPs in mtDNA and nDNA, the count of 5'-ends of all paired-end and single-end alignments were determined for all samples and shifted one base upstream to the location of the free 5'-end or hydrolysed rNMP. The read data were normalized by dividing the reads for each individual rNMP by the strand-specific genome content of its dNMP counterpart. Subsequently, the strand-specific relative proportions of the four rNMPs or 5'-ends were calculated as a percentage. Finally, the percentages for the two DNA strands were averaged to generate the numbers representing the genome as a whole.

Nucleotide pool measurement

For nucleotide pool measurements, mouse embryos, and spleens and skeletal muscle from adult mice (aged 13 weeks) were isolated as described above, rapidly placed in 700 µl ice-cold 12% (w/v) TCA and 15 mM $MgCl_2$, frozen in liquid nitrogen and stored at -80°C. Nucleotide extraction was performed as described previously [28], and sample clean-up over solid-phase extraction columns and high-performance liquid chromatography was carried out as described previously [27,53].

References

1 Gorman GS, Chinnery PF, DiMauro S, Hirano M, Koga Y, McFarland R, Suomalainen A, Thorburn DR, Zeviani M & Turnbull DM (2016) Mitochondrial diseases. 1–22.

2 Pikó L, Hougham AJ & Bulpitt KJ (1988) Studies of sequence heterogeneity of mitochondrial DNA from rat and mouse tissues: evidence for an increased frequency of deletions/additions with aging. *Mech. Ageing Dev.* **43**, 279–293.

3 Cortopassi GA & Arnheim N (1990) Detection of a specific mitochondrial DNA deletion in tissues of older humans. *Nucleic Acids Res* **18**, 6927–6933.

4 Kennedy SR, Salk JJ, Schmitt MW & Loeb LA (2013) Ultra-Sensitive Sequencing Reveals an Age-Related Increase in Somatic Mitochondrial Mutations That Are Inconsistent with Oxidative Damage. *PLoS Genet* **9**, e1003794–10.

5 Pinto M & Moraes CT (2015) Mechanisms linking mtDNA damage and aging. *Free Radic. Biol. Med.* **85**, 250–258.

6 Nick McElhinny SA, Watts BE, Kumar D, Watt DL, Lundström E-B, Burgers PMJ, Johansson E, Chabes A & Kunkel TA (2010) Abundant ribonucleotide incorporation into DNA by yeast replicative polymerases. *Proc Natl Acad Sci USA* **107**, 4949–4954.

7 Nick McElhinny SA, Kumar D, Clark AB, Watt DL, Watts BE, Lundström E-B, Johansson E, Chabes A & Kunkel TA (2010) Genome instability due to ribonucleotide incorporation into DNA. *Nat. Chem. Biol.* **6**, 774–781.

8 Li Y & Breaker RR (1999) Kinetics of RNA degradation by specific base catalysis of transesterification involving the 2γ-hydroxyl group. *Journal of the American Chemical Society* **121**, 5364–5372.

9 Jaishree TN, van der Marel GA, van Boom JH & Wang AH (1993) Structural influence of RNA incorporation in DNA: quantitative nuclear magnetic resonance refinement of d(CG)r(CG)d(CG) and d(CG)r(C)d(TAGCG). *Biochemistry* **32**, 4903–4911.

10 Chiu H-C, Koh KD, Evich M, Lesiak AL, Germann MW, Bongiorno A, Riedo E & Storici F (2014) RNA intrusions change DNA elastic properties and structure. *Nanoscale* **6**, 10009–10017.

11 DeRose EF, Perera L, Murray MS, Kunkel TA & London RE (2012) Solution Structure of the Dickerson DNA Dodecamer Containing a Single Ribonucleotide. *Biochemistry* **51**, 2407–2416.

12 Sparks JL, Chon H, Cerritelli SM, Kunkel TA, Johansson E, Crouch RJ & Burgers PM (2012) RNase H2-initiated ribonucleotide excision repair. *Mol Cell* **47**, 980–986.

13 Reijns MAM, Rabe B, Rigby RE, Mill P, Astell KR, Lettice LA, Boyle S, Leitch A, Keighren M, Kilanowski F, Devenney PS, Sexton D, Grimes G, Holt IJ, Hill RE, Taylor MS, Lawson KA, Dorin JR & Jackson AP (2012) Enzymatic removal of ribonucleotides from DNA is essential for mammalian genome integrity and development. *Cell* **149**, 1008–1022.

14 Hiller B, Achleitner M, Glage S, Naumann R, Behrendt R & Roers A (2012) Mammalian RNase H2 removes ribonucleotides from DNA to maintain genome integrity. *Journal of Experimental Medicine* **209**, 1419–1426.

15 Wanrooij PH & Chabes A (2019) Ribonucleotides in mitochondrial DNA. *FEBS Lett* **121**, 5364.

16 Forslund JME, Pfeiffer A, Stojkovič G, Wanrooij PH & Wanrooij S (2018) The presence of rNTPs decreases the speed of mitochondrial DNA replication. *PLoS Genet* **14**, e1007315.

17 Kasiviswanathan R & Copeland WC (2011) Ribonucleotide Discrimination and Reverse Transcription by the Human Mitochondrial DNA Polymerase. *Journal of Biological Chemistry* **286**, 31490–31500.

18 Göksenin AY, Zahurancik W, LeCompte KG, Taggart DJ, Suo Z & Pursell ZF (2012) Human DNA polymerase ε is able to efficiently extend from multiple consecutive ribonucleotides. *Journal of Biological Chemistry* **287**, 42675–42684.

19 Wanrooij PH, Engqvist MKM, Forslund JME, Navarrete C, Nilsson AK, Sedman J, Wanrooij S, Clausen AR & Chabes A (2017) Ribonucleotides incorporated by the yeast mitochondrial DNA polymerase are not repaired. *Proc. Natl. Acad. Sci. U.S.A.* **114**, 12466–12471.

20 Berglund A-K, Navarrete C, Engqvist MKM, Hoberg E, Szilagyi Z, Taylor RW, Gustafsson CM, Falkenberg M & Clausen AR (2017) Nucleotide pools dictate the identity and frequency of ribonucleotide incorporation in mitochondrial DNA. *PLoS Genet* **13**, e1006628.

21 Moss CF, Rosa ID, Hunt LE, Yasukawa T, Young R, Jones AWE, Reddy K, Desai R, Virtue S, Elgar G, Voshol P, Taylor MS, Holt IJ, Reijns MAM & Spinazzola A (2017) Aberrant ribonucleotide incorporation and multiple deletions in mitochondrial DNA of the murine MPV17 disease model. *Nucleic Acids Res* **45**, 12808–12815.

22 Pikó L & Matsumoto L (1977) Complex forms and replicative intermediates of mitochondrial DNA in tissues from adult and senescent mice. *Nucleic Acids Res* **4**, 1301–1314.

23 Pohjoismäki JLO, Goffart S, Tyynismaa H, Willcox S, Ide T, Kang D, Suomalainen A, Karhunen PJ, Griffith JD, Holt IJ & Jacobs HT (2009) Human heart mitochondrial DNA is organized in complex catenated networks containing abundant four-way junctions and replication forks. *J. Biol. Chem.* **284**, 21446–21457.

24 Grossman LI, Watson R & Vinograd J (1973) The presence of ribonucleotides in mature closed-circular mitochondrial DNA. *Proc. Natl. Acad. Sci. U.S.A.* **70**, 3339–3343.

25 Wong-Staal F, Mendelsohn J & Goulian M (1973) Ribonucleotides in closed circular mitochondrial DNA from HeLa cells. *Biochem Biophys Res Commun* **53**, 140–148.

26 Miyaki M, Koide K & Ono T (1973) RNase and alkali sensitivity of closed circular mitochondrial DNA of rat ascites hepatoma cells. *Biochem Biophys Res Commun* **50**, 252–258.

27 Kong Z, Jia S, Chabes AL, Appelblad P, Lundmark R, Moritz T & Chabes A (2018) Simultaneous determination of ribonucleoside and deoxyribonucleoside triphosphates in biological samples by hydrophilic interaction liquid chromatography coupled with tandem mass spectrometry. *Nucleic Acids Res* **57**, 349–8.

28 Rentoft M, Lindell K, Tran P, Chabes AL, Buckland RJ, Watt DL, Marjavaara L, Nilsson AK, Melin B, Trygg J, Johansson E & Chabes A (2016) Heterozygous colon cancer-associated mutations of SAMHD1 have functional significance. *Proc Natl Acad Sci USA* **113**, 4723–4728.

29 Behrendt R, Schumann T, Gerbaulet A, Nguyen LA, Schubert N, Alexopoulou D, Berka U, Lienenklaus S, Peschke K, Gibbert K, Wittmann S, Lindemann D, Weiss S, Dahl A, Naumann R, Dittmer U, Kim B, Mueller W, Gramberg T & Roers A (2013) Mouse SAMHD1 has antiretroviral activity and suppresses a spontaneous cell-intrinsic antiviral response. *Cell Rep* **4**, 689–696.

30 Clausen AR, Lujan SA, Burkholder AB, Orebaugh CD, Williams JS, Clausen MF, Malc EP, Mieczkowski PA, Fargo DC, Smith DJ & Kunkel TA (2015) Tracking replication enzymology in vivo by genome-wide mapping of ribonucleotide incorporation. *Nat Struct Mol Biol* **22**, 185–191.

31 Johnson PH & Laskowski M (1970) Mung bean nuclease I. II. Resistance of double stranded deoxyribonucleic acid and susceptibility of regions rich in adenosine and thymidine to enzymatic hydrolysis. *J. Biol. Chem.* **245**, 891–898.
32 Kowaltowski AJ, de Souza-Pinto NC, Castilho RF & Vercesi AE (2009) Mitochondria and reactive oxygen species. *Free Radic. Biol. Med.* **47**, 333–343.
33 López-Otín C, Blasco MA, Partridge L, Serrano M & Kroemer G (2013) The Hallmarks of Aging. *Cell* **153**, 1194–1217.
34 KRISHNAN KJ, GREAVES LC, REEVE AK & Turnbull DM (2007) Mitochondrial DNA Mutations and Aging. *Annals of the New York Academy of Sciences* **1100**, 227–240.
35 Larsson N-G (2010) Somatic mitochondrial DNA mutations in mammalian aging. *Annu Rev Biochem* **79**, 683–706.
36 Trifunovic A, Wredenberg A, Falkenberg M, Spelbrink JN, Rovio AT, Bruder CE, Bohlooly-Y M, Gidlöf S, Oldfors A, Wibom R, Törnell J, Jacobs HT & Larsson N-G (2004) Premature ageing in mice expressing defective mitochondrial DNA polymerase. *Nature* **429**, 417–423.
37 Kujoth GC, Hiona A, Pugh TD, Someya S, Panzer K, Wohlgemuth SE, Hofer T, Seo AY, Sullivan R, Jobling WA, Morrow JD, Van Remmen H, Sedivy JM, Yamasoba T, Tanokura M, Weindruch R, Leeuwenburgh C & Prolla TA (2005) Mitochondrial DNA mutations, oxidative stress, and apoptosis in mammalian aging. *Science* **309**, 481–484.
38 Vermulst M, Wanagat J, Kujoth GC, Bielas JH, Rabinovitch PS, Prolla TA & Loeb LA (2008) DNA deletions and clonal mutations drive premature aging in mitochondrial mutator mice. *Nature Genetics* **40**, 392–394.
39 Franzolin E, Pontarin G, Rampazzo C, Miazzi C, Ferraro P, Palumbo E, Reichard P & Bianchi V (2013) The deoxynucleotide triphosphohydrolase SAMHD1 is a major regulator of DNA precursor pools in mammalian cells. *Proc Natl Acad Sci USA* **110**, 14272–14277.
40 Lakshmipathy U & Campbell C (2001) Antisense-mediated decrease in DNA ligase III expression results in reduced mitochondrial DNA integrity. *Nucleic Acids Res* **29**, 668–676.
41 Puebla-Osorio N, Lacey DB, Alt FW & Zhu C (2006) Early embryonic lethality due to targeted inactivation of DNA ligase III. *Molecular and Cellular Biology* **26**, 3935–3941.
42 Lakshmipathy U & Campbell C (1999) The human DNA ligase III gene encodes nuclear and mitochondrial proteins. *Molecular and Cellular Biology* **19**, 3869–3876.
43 Gao Y, Katyal S, Lee Y, Zhao J, Rehg JE, Russell HR & McKinnon PJ (2011) DNA ligase III is critical for mtDNA integrity but not Xrcc1-mediated nuclear DNA repair. *Nature* **471**, 240–244.
44 Simsek D, Furda A, Gao Y, Artus J, Brunet E, Hadjantonakis A-K, Van Houten B, Shuman S, McKinnon PJ & Jasin M (2011) Crucial role for DNA ligase III in mitochondria but not in Xrcc1-dependent repair. *Nature* **471**, 245–248.
45 Leandro GS, Sykora P & Bohr VA (2015) The impact of base excision DNA repair in age-related neurodegenerative diseases. *Mutat. Res.* **776**, 31–39.
46 Akbari M, Keijzers G, Maynard S, Scheibye-Knudsen M, Desler C, Hickson ID & Bohr VA (2014) Overexpression of DNA ligase III in mitochondria protects cells against oxidative stress and improves mitochondrial DNA base excision repair. *DNA Repair* **16**, 44–53.
47 Chen D, Cao G, Hastings T, Feng Y, Pei W, O'Horo C & Chen J (2002) Age-dependent decline of DNA repair activity for oxidative lesions in rat brain mitochondria. *J. Neurochem.* **81**, 1273–1284.

48 Imam SZ, Karahalil B, Hogue BA, Souza-Pinto NC & Bohr VA (2006) Mitochondrial and nuclear DNA-repair capacity of various brain regions in mouse is altered in an age-dependent manner. *Neurobiol. Aging* **27**, 1129–1136.

49 Srivastava S (2017) The Mitochondrial Basis of Aging and Age-Related Disorders. *Genes* **8**, 398–23.

50 Sambrook J & Russell DW (2001) *Molecular Cloning*, 3rd ed. CSHL Press.

51 Ahola-Erkkilä S, Carroll CJ, Peltola-Mjösund K, Tulkki V, Mattila I, Seppänen-Laakso T, Oresic M, Tyynismaa H & Suomalainen A (2010) Ketogenic diet slows down mitochondrial myopathy progression in mice. *Human molecular genetics* **19**, 1974–1984.

52 Pfaffl MW (2001) A new mathematical model for relative quantification in real-time RT-PCR. *Nucleic Acids Research* **29**, e45.

53 Jia S, Marjavaara L, Buckland R, Sharma S & Chabes A (2015) Determination of deoxyribonucleoside triphosphate concentrations in yeast cells by strong anion-exchange high-performance liquid chromatography coupled with ultraviolet detection. *Methods Mol Biol* **1300**, 113–121.

Figure 1

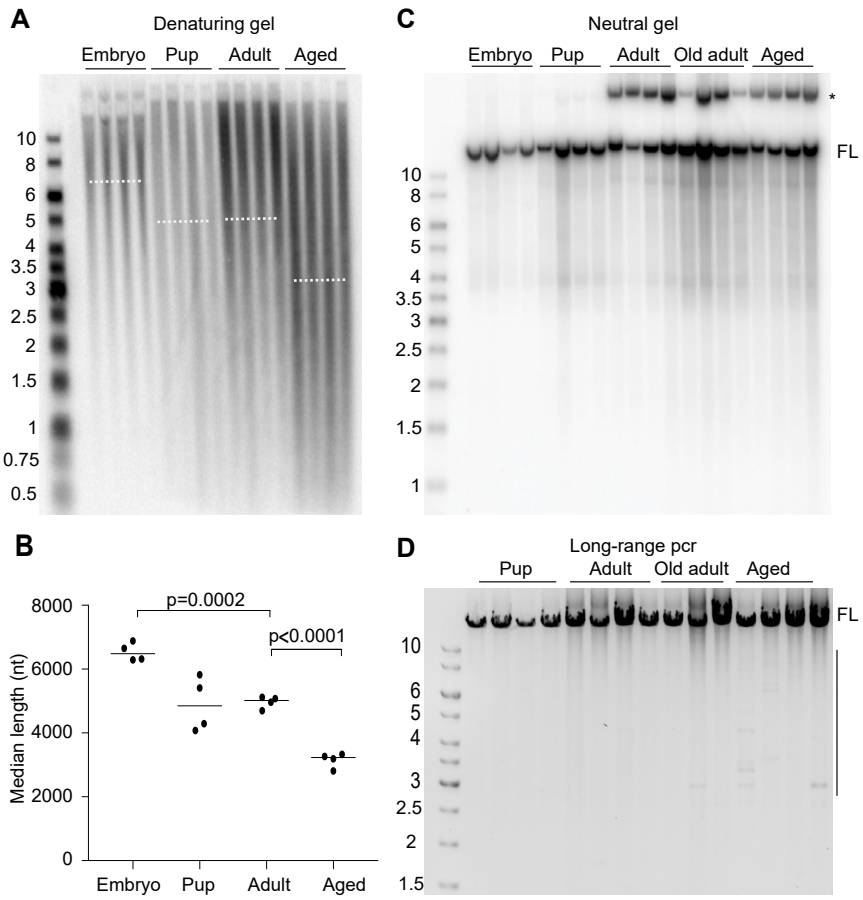

Figure 2

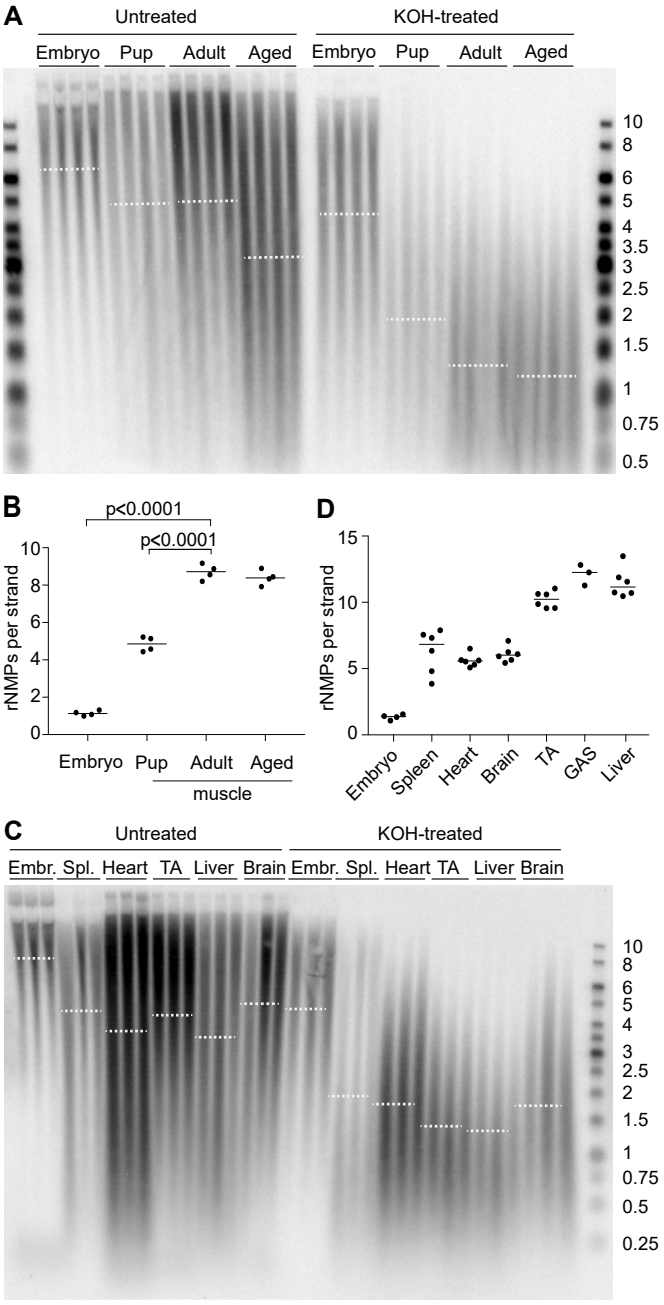

Figure 3

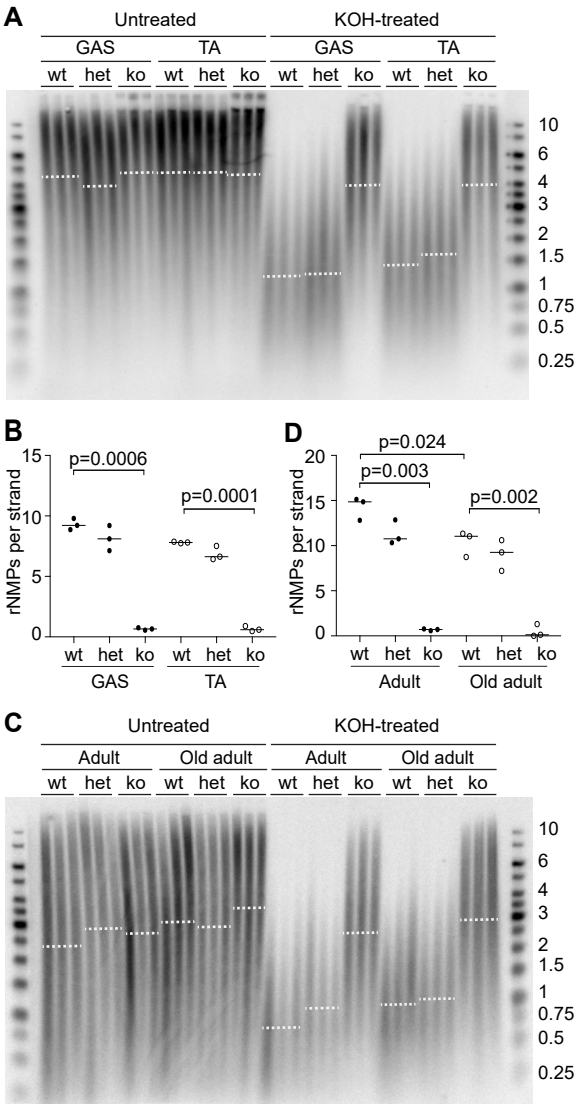

Figure 4

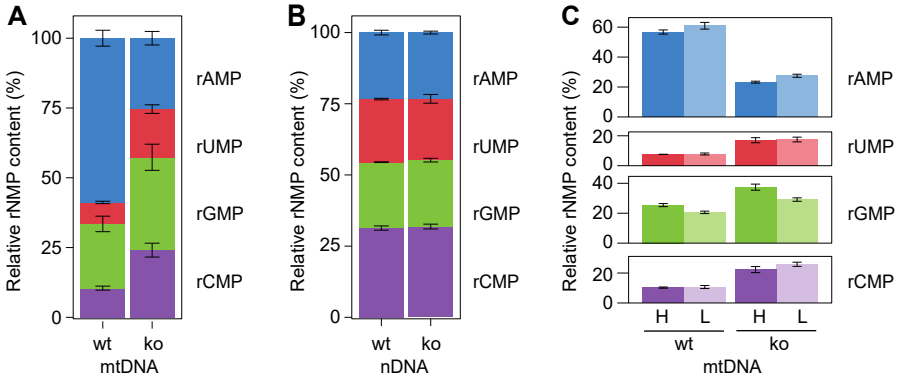

Figure 5

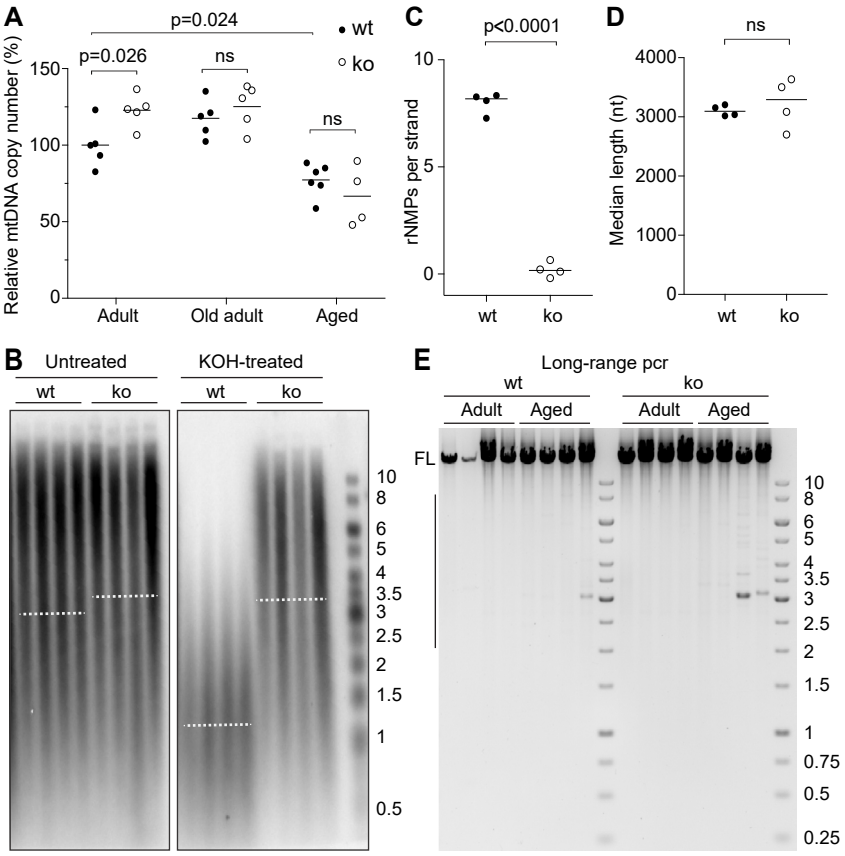

Figure 6